Proceedings of the NUMETA '85 Conference / Swansea / 7-11 January 1985

Numerical analysis of flexible retaining walls

J.W.PAPPIN, B.SIMPSON, P.J.FELTON & C.RAISON
Ove Arup & Partners, London, UK

ABSTRACT: A numerical method for analysing the behaviour of flexible retaining walls is presented. The method differs significantly from the traditional subgrade reaction approach in the ways that the soil stiffness and earth pressure limits are modelled. Three stiffness matrices are used in the analysis which allows soil-structure interaction to be modelled. One matrix represents the wall in bending while the other two represent the soil on each side of the wall. Each soil stiffness matrix is assembled using two pre-calculated flexibility matrices obtained from finite element analyses of elastic soil blocks. Earth pressure limits are determined from consideration of forces applied to the soil which allows the known effect of soil arching to be modelled. This occasionally permits pressures to locally exceed active and passive limits. The analysis has been incorporated into a computer program which is sufficiently economic and simple enough to be used as part of the general design process. Examples of its use are given.

1 INTRODUCTION

The term "flexible retaining walls" includes sheet pile walls, diaphragm (slurry, trench) walls, and secant pile walls. They are usually associated with excavations and support the ground adjacent to the excavation by transmitting horizontal earth pressures either into struts and anchors or into the soil at greater depth. The design of flexible retaining walls requires an assessment of the necessary penetration of the wall, the bending moments and shear forces to be resisted by the wall and the movements of the wall and the adjacent soil.

Traditionally, the design of these walls has been carried out using stability considerations combined with empirical rules to determine movements, bending moments and shear forces. While this is usually adequate to determine the necessary penetration, the empirical methods are often not sufficiently accurate and in some cases are not applicable. The wall movements, bending moments and shear forces are very dependent on the stiffnesses of the wall, struts and the soil. In addition, the stress changes applied to the soil frequently give rise to plastic failure within parts of the soil.

Satisfactory mathematical modelling of the behaviour of this soil structure system generally involves the use of a non linear finite element analysis method. For routine analysis by general designers finite elements methods tend to be expensive and complex and therefore susceptible to error. Consequently a simpler analysis system is desirable.

This paper describe an alternative method of analysis that is sufficiently simple and inexpensive that it can form part of the general design process. As with finite element computations the analysis is carried out in steps corresponding to the stages of the construction. The analysis can accommodation the following parameters:

- soil layering including different materials each side of the wall
- limits to the problem including a rigid base and vertical boundaries (e.g. the centre line of a trench).
- pore water pressure which can either be hydrostatic or directly specified.
- surcharges, either uniformly distributed loads or strip loads.
- excavation/filling, soil can be added or removed from either side of the wall
- anchors or struts can be installed or removed at any stage.

It is recognised that there are many

computer programs available which incorporate analysis methods for this type of problem. The method of analysis presented here, however, differs significantly from these in the way the soil is modelled. The analysis method has been incorporated into a computer program for general use in a design office and various examples are given. Some shortcomings of the analysis are discussed.

2 DESCRIPTION OF THE ANALYSIS

Figure 1 shows typical stages of construction that the analysis can model. At each stage the incremental displacements due to the changes caused by that stage are calculated and added to the existing displacements. The soil stresses, strut forces, wall bending moments and shear forces can then be determined.

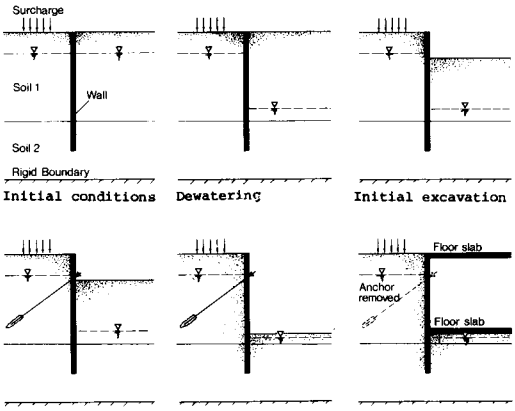

Fig 1. Typical stages of construction

2.1 Numerical Representation

The numerical representation is shown on Figure 2. The wall is modelled as a series of elastic beam elements joined at the nodes. Depending on the method used to characterise the soil stiffness the lowest node is either the base of the wall or at a prescribed rigid base in the ground beneath the wall. The soil to each side of the wall is connected at the nodes as shown on the figure. Only horizontal forces can be transmitted between the soil and the nodes and these forces are directly related to the earth pressures. Struts or anchors are modelled as forces and spring stiffnesses connected to the relevant nodes.

The analysis assumes plane strain conditions throughout except when the Mindlin method is used to represent soil stiffness as described in section 2.4.

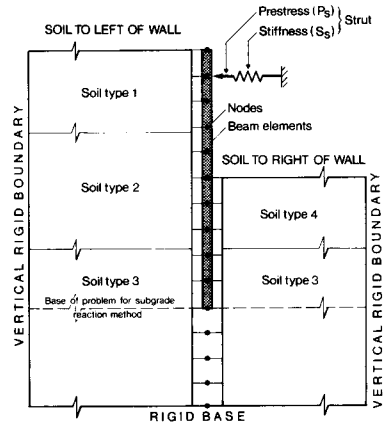

Fig 2. Numerical representation

2.2 Method of Analysis

At each stage of construction the analysis comprises the following steps.

(a) The initial earth pressures and the out of balance nodal forces are calculated assuming no movement of the nodes.

(b) Stiffness matrices representing the soil on either side of the wall and the wall itself are assembled.

(c) These matrices are combined together with any stiffnesses representing the actions of struts or anchors to form an overall stiffness matrix.

(d) The incremental nodal displacements are calculated from the nodal forces acting on the overall stiffness matrix assuming linear elastic behaviour.

(e) The earth pressures at each node are calculated by adding the changes in earth pressure due to the current stage to the initial earth pressures. The derivation of the changes in earth pressure includes multiplying the incremental nodal displacements by the soil stiffness matrices.

(f) The earth pressures are compared with soil strength limitation criteria conventionally taken as either the active or passive limits. If any strength criterion is infringed a set of nodal correction forces is calculated. These forces are used to restore earth pressures which are consistent with the strength criteria and also model the consequent plastic deformation within the soil.

(g) A new set of nodal forces is calculated by adding the nodal correction

forces to those calculated in step (a).

(h) Steps (d) to (g) are repeated until convergence is achieved.

(i) Total nodal displacements, earth pressures, strut forces and wall shear stresses and bending moments are calculated.

Details of the above steps are given in relation to each of the principal variables in the following sections.

2.3 Wall Stiffness

The wall is modelled as a series of elastic beam elements. The stiffness matrix is derived using conventional methods from slope deflection equations as follows.

The moments [M] and horizontal forces [P] at the nodes are represented as

$$[M] = [A][\delta] + [B][\Theta]$$

$$\text{and} \quad [P] = [C][\delta] + [A]^T[\Theta] \qquad (1)$$

where [A], [B] and [C] are functions of the element lengths and flexural rigidity (EI); $[\delta]$ are the nodal horizontal displacements and $[\Theta]$ are the nodal rotations.

As there are no moments applied to the wall $[\Theta]$ can be eliminated to give

$$[P] = [[C] - [A]^T[B]^{-1}[A]]\ [\delta] \text{ or}$$
$$[P] = [S][\delta] \qquad (2)$$

in which [S] is the wall stiffness matrix.

2.4 Soil Stiffness

The formulation of a stiffness matrix to model the soil is not as straightforward as that used for the wall. The program provides three alternative methods to the designer.

(a) Subgrade reaction model

The soil is represented by individual linear elastic springs connected to the wall at the node points as shown in Figure 3. The stiffnesses in terms of force per unit displacement per unit length of spring and lengths of the springs are specified to represent the soil at each node. The length and stiffness values are closely associated and their selection is difficult because they are not basic soil parameters.

A major weakness is that the soil nodal displacements are not interconnected. If one node is acted on by a force then only that node responds whereas the adjacent nodes are not moved. This is clearly not representative of real soil behaviour. Design rules for the choice of length and stiffness can only be formulated once the likely behaviour is known. This is not very satisfactory and implies that ideally the soil stiffnesses should be modified

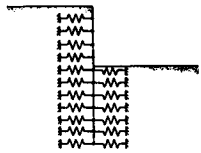

Fig 3. Subgrade reaction model

within the analysis for each stage of the construction.

Nevertheless, the subgrade reaction model can be very useful for analysing specific types of non standard problems. For example, it is considered that horizontally loaded piles can be satisfactorily modelled using this model.

(b) Finite Element flexibility model

In this method the soil on each side of the wall is modelled as a block of elastic material. The behaviour of each elastic block is represented by a stiffness matrix which is obtained by inverting a flexibility matrix derived as follows.

Finite element analyses have previously been carried out for the block of material shown in Figure 4. Flexibility matrices for load on the vertical surface AB have been stored for two different elastic blocks. These flexibility matrices define the magnitude of the horizontal displacements at all the nodes on the vertical free surface due to a unit load applied at any one node. Plane strain conditions were assumed. The two different cases of elastic blocks used were uniform Young's modulus and Young's modulus increasing linearly with depth from zero at the surface.

The flexibility matrices from the two cases are combined proportionally to cover any situation in which stiffness increases linearly with depth, whatever the value at

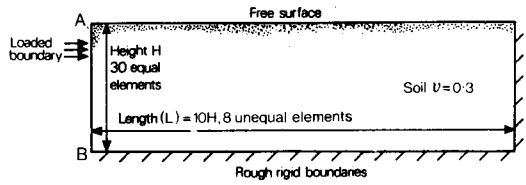

Fig 4. Soil block used in finite element analysis

the free surface. No theoretical basis has been found to confirm that such a combination would give an accurate result, but comparison with further finite element studies suggests that the approximation is, in fact, very good.

The program manipulates the flexibility matrix to generate an equivalent flexibility matrix compatible with the node spacing used to represent the wall. This manipulation is achieved by scaling the finite element mesh to match the height of the elastic soil block and then linearly combining the flexibility terms to produce the desired matrix. Special attention has been paid to achieving good approximations for the dominant terms on the leading diagonal of the matrix.

Linear variation of stiffness with depth can oversimplify the design profile. An approximate method of adjusting the matrices to accommodate non-linear variations of soil stiffness is outlined below.

To represent E_z, the variation of Young's modulus with depth (z), a best fit linear approximation E^*_z is first calculated. The flexibility matrix [F*] corresponding to E^*_z is derived as described above. The following ratio is calculated for each node.

$$\int_{z=0}^{D} \frac{E^{*2}_z}{E_z} \left(\frac{\partial \delta^*_{iz}}{\partial z}\right) dz \Bigg/ \int_{z=0}^{D} E^*_z \left(\frac{\partial \delta^*_{iz}}{\partial z}\right) dz \qquad (3)$$

where δ^*_{iz} is the flexibility at depth z resulting from unit load applied at node i calculated using the assumed modulus E^*_z. D is the depth to the rigid boundary.

The flexibility matrix [F], corresponding to the original variation E_z, is determined by multiplying each row in [F*] by the appropriate ratio. Terms representing the effect of a unit load at node i are multiplied by the ratio calculated for node i. Symmetry is maintained by using the minimum flexibility produced for each pair of nodes. Figure 5 shows a comparison of the "correct" finite element solution and that produced by this approximation. The problem illustrated is one of the more severe cases that could be envisaged: Other comparisons with matrices developed by a finite element studies indicate that, for practical situations, errors will rarely exceed 20%.

The flexibility matrices were derived for one specific geometry which represented a length to height (L/H) ratio of 10 (see Figure 4). As L/H changes, the flexibility matrix will change and hence the stiffness matrix. To allow for varying L/H ratios the stiffness matrix has been further modified by adding a single spring at each node point. For high L/H ratios the spring stiffness is small due to the large spring length and the stiffness matrix is virtually unchanged. For small L/H ratios the single spring stiffness becomes dominant and controls the calculated wall movements. Test comparisons were carried out with finite elements (for an elastic soil which had a linearly increasing stiffness with depth) to determine the error due to this simplified assumption. The agreement was within 10 % for L/H ratios in the range 0.3 to 0.6 and for L/H ratios greater than about 3. The largest differences occur for L/H ratios of about 1 when the maximum difference between the two methods is about 30 %.

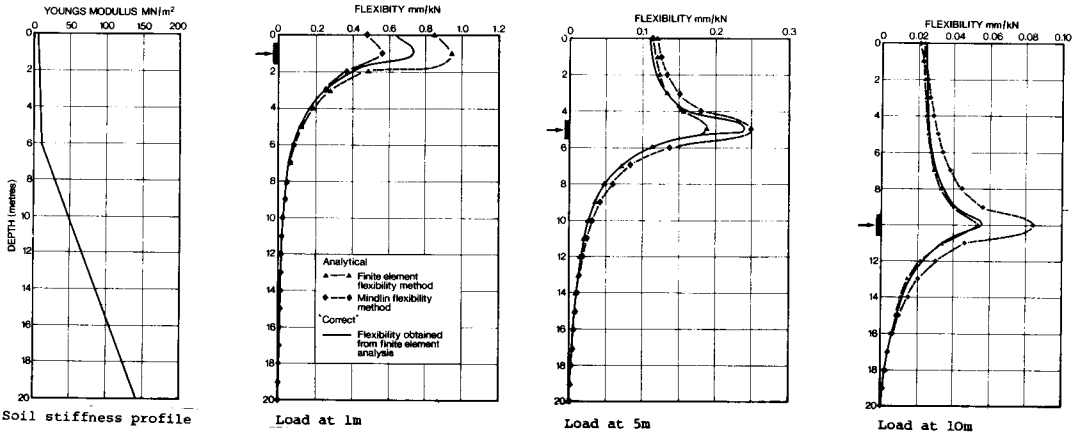

Fig. 5. Comparison of flexibility approximations at three depths

(c) Mindlin flexibility method

This method is very similar to the finite element flexibility method in that the soil is modelled as blocks of elastic material. The method uses the integrals of the Mindlin equations which were published by Vaziri et. al. (1982). The integrals calculate the displacement at any point due to either a vertical or horizontal stress applied to either a vertical or horizontal rectangular area within an elastic half space. If there is no rigid base or vertical loading they can be used directly to determine the flexibility coefficients of the nodal points due to horizontal pressures applied to the nodes. The flexibility of the soil on each side of the wall is equal to twice that of a half space. This is due to the absence of the effect of the soil on one side of the wall assuming that the wall is at a plane of symmetry. The effect of the width, or out of plane dimension of the retaining wall can also be taken into account to some extent as the equations model the length of the pressure loaded rectangular area in the out of plane direction. Clearly if this dimension is large a plane strain condition is modelled.

The soil being modelled is not an elastic half space, however, and the effects of the assumed rigid base and vertical boundary should ideally be incorporated. To take these boundaries into account additional nodes are included when formulating the flexibility matrix (see Figure 6). When modelling each side of the wall the soil must still be considered as a half space and the resulting flexibility matrix doubled. Therefore to maintain symmetry at the plane of the wall additional nodes must be added to both sides. The base nodes are restrained both vertically (Z-Z direction) and horizontally (X-X) whereas the vertical boundary nodes are only restrained horizontally (X-X). As these nodes are on a plane of symmetry (X-X, Z-Z) they will not move in the Y-Y direction.

Nodal restraints are achieved by modelling stresses acting on rectangular areas centred at each node to force the displacements of the nodes to be zero. For a vertical boundary node a horizontal pressure is considered to act on a vertical rectangle. For a base node two stresses are considered, one being a horizontal traction and the other a vertical pressure, both acting on a horizontal rectangle. In all cases the width of the rectangle is taken as being

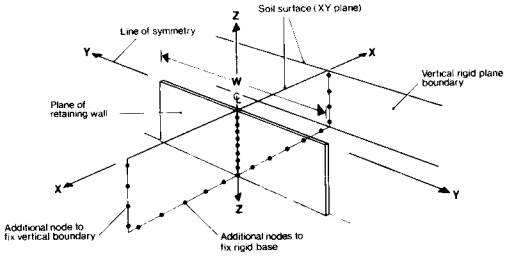

Fig 6. Half space representation of soil block

equal to the width (W) specified for the wall.

The final soil stiffness matrix can be computed by eliminating the fixed nodes and inverting the flexibility matrix of the central nodes only.

This method of modelling fixity is considered to be reasonable when W is large relative to the depth or to the distance to the vertical boundary. When W is small three dimensional effects will dominate and to approximate the fixity of a plane by a single line of nodes becomes somewhat dubious. Additional nodes on the fixed planes away from the plane of symmetry (X-X, Z-Z), or varying the width (W) of the loaded rectangle at the fixed nodes would improve this approximation. Nevertheless using the Mindlin flexibility method provides approximate means of studying the importance of W.

A drawback of the Mindlin flexibility method is that Young's modulus is assumed to be constant with depth. This is significantly different from the finite element flexibility method which can model accurately a linearly increasing modulus with depth. Nevertheless the same ratios that are applied to model modulus variations (Equation 3) can still be used with the Mindlin method. An example comparing flexibility coefficients is given in Figure 5 where it can be seen that the approximation is quite good.

(d) Comparison of methods

The subgrade reaction method is significantly different from the finite element and Mindlin flexibility methods. This is illustrated for a strutted sheet pile wall in a sand in Figure 7. It can be seen that the subgrade reaction model fails to detect the increase in earth pressure in the vicinity of the strut. This leads to a considerable under-estimate of the strut force and a slight over-estimate of the bending moments in the wall.

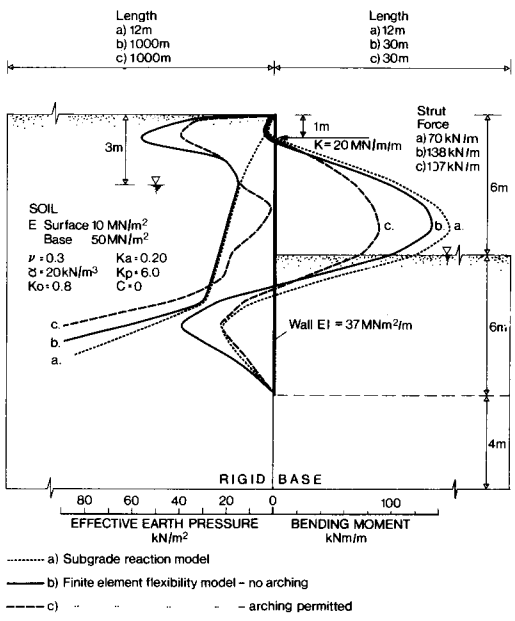

Fig 7. Comparison of soil models

The finite element and Mindlin flexibility methods behave similarly. The Mindlin flexibility method is more tolerant of very uneven node spacing but the finite element flexibility method is generally better when variations of Young's modulus with depth are to be modelled. Both methods assume a constant Poisson's ratio (ν) and the finite element flexibility method has only been established with a value of 0.3 The facility to model restricted width in the out of plane direction in the Mindlin method is promising but is not fully developed as yet and is difficult to check against any other type of analysis.

2.5 Soil strength limitations

The soil strength limitations are modelled using active and passive pressure states

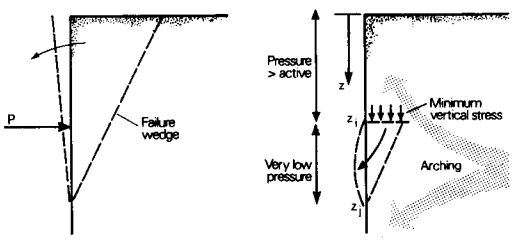

Fig 8. Mechanism for active failure

which may be represented at any depth z by

$$p_a < p < p_p \qquad (4)$$

where:

p = earth pressure

$p_a = K_a p'_v - K_{ac} c + u$ = active earth pressure

$p_p = K_p p'_v + K_{pc} c + u$ = passive earth pressure

and K_a, K_p, K_{ac}, K_{pc} = earth pressure coefficients at depth z

p'_v = vertical effective stress

c = cohesion

u = pore water pressure

In the absence of wall friction and adhesion, Inequality (4) corresponds to a Rankine analysis. It can be shown that Inequality (4) represents a sufficient condition for stability of the soil, but not a necessary condition. In many circumstances, it is possible for the earth pressure at some points on the wall to lie outside these limits without the formation of a mechanism.

The formation of a mechanism can be studied by analysis of a wedge of soil, as shown in Figure 8a. Coulomb showed that, in the absence of wall friction, the force P between ground surface and depth z was limited thus:

$$\int_o^z p_a \, dz \leqslant P = \int_o^z p dz \leqslant \int_o^z p_p \, dz \qquad (5)$$

The notation here is as in Inequality (4). Inequality (5) provides necessary conditions for the prevention of a mechanism which extends from depth z up to the ground surface. It is not, however, sufficient to prevent other localised mechanisms developing within the soil body.

In order to provide a good approximation to conditions which are both necessary and sufficient to prevent instability, the mechanism represented by Figure 8b has been studied. It is considered that this type of mechanism will not occur provided that at any depth z_j:

$$\int_{z_i}^{z_j} p_{az} \, dz \leqslant \int_{z_i}^{z_j} p dz \leqslant \int_{z_i}^{z_j} p_{pz} \, dz \qquad (6)$$

for all $z_i < z_j$

where: p_{az} at depth z ($z_i < z < z_j$) is set equal to

$$K_a\left(\sigma'_{vi\ min} + \int_{z_i}^{z}\gamma dz - u + u_i\right) - K_{ac}c + u \quad (7)$$

and $\sigma'_{vi\ min}$ is the minimum vertical effective stress which could occur at depth z_i.

u_i is the pore pressure at depth z_i. Similarly p_{pz} at depth z is set equal to

$$K_p\left(\sigma'_{vi\ max} + \int_{z}^{z_i}\gamma dz - u + u_i\right) + K_{pc}\,c + u \quad (8)$$

where: $\sigma'_{vi\ max}$ is the maximum vertical effective stress which could occur at depth z_i.

The minimum and maximum vertical effective stresses are not necessarily equal to the vertical effective stress induced by the overburden and surcharges. If arching occurs the vertical stress on the soil adjacent to the wall may vary greatly. If wall friction is ignored, however, the minimum and maximum vertical stresses at depth z_i are taken as being equal to

$$\sigma'_{vi\ min} = p'_i\ K_{ai} - K_{aci}\,c_i \quad \text{and}$$
$$\sigma'_{vi\ max} = p'_i\ K_{pi} + K_{pci}\,c_i \quad (9)$$

where p'_i is the horizontal effective stress acting at depth z_i and K_{ai}, K_{pi}, K_{aci}, K_{pci} and c_i are the earth pressure coefficients and the cohesion at depth z_i. These equations provide an approximate method of representing local failure of the soil. Use of conditions (6) to (9) provides a conservative limitation on the amount of arching which can occur.

The designer may choose whether to use Inequality (4) or Inequality (6). It is believed that Inequality (6) is more reasonable and better reflects the actual situation as it permits a limited degree of arching to occur within the soil body. The effect of this choice is clearly illustrated in Figure 7 where the results using Inequality (4) are referred to as 'no arching' and the results using Inequality (6) are referred to as 'arching permitted'. As the earth pressures near the strut are well above active pressure (p > pa) the analysis using Inequality (6) has permitted the pressures at greater depth to reduce below the Rankine active pressure. This has markedly reduced the bending moments in the wall and the strut force.

To ensure that the active and passive pressure limits evaluated above are not violated, the program computes nodal correction forces to restore acceptable pressure levels. To obtain convergence reliably it has been found necessary to achieve this by way of a set of "displacement corrections" from which the force corrections are calculated using the soil flexibility matrix. The "displacement corrections" are computed for each node and are associated with the plastic strain developed in the body of soil.

When "displacement corrections" are used the earth pressure at any node is still influenced through the soil flexibility by the movement of the nodes below. However the earth pressure may be independent of the movement of the node itself and nodes above. For example, consider an active or passive failure as shown in Figure 9. The "displacement correction" applied to ensure that the limits are not violated at node q will cause a change of pressure but no displacement at node r, whilst at node p there will be a change of displacement but no change of pressure. This means that movement is taking place at constant stress on the failure surface whilst elastic conditions are still maintained separately in the blocks of material on either side of the failure surface.

To satisfy the above conditions the "displacement corrections" are calculated using the following procedure which works downwards through each node starting at the free surface.

(a) at the node (labelled here as i for convenience) calculate the approximate displacement correction that would cause the pressure at the node to change by the required amount to comply with the strength criteria.

(b) For each node j above node i calculate the displacement correction that is required to prevent a change of pressure at node j when the displacement at node i is corrected by the approximate displacement correction.

(c) Having completed (a) and (b) for all the nodes sum the displacement corrections to determine the total "displacement correction" for each node.

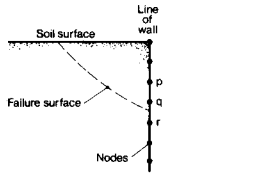

Fig 9. Failure surface in soil.

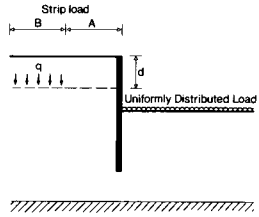

Fig 10. Surcharge geometry

2.6 Excavation or Filling

The effect of excavation or filling is modelled by specifying the stress ratio of change in horizontal effective stress over change in vertical effective stress. This ratio is denoted by K_o and K_r which are used by the analysis as follows:

(a) K_o for determining the horizontal effective stress in either the initialisation stage or in filled material, and

(b) K_r for determing the change in horizontal effective stress due to a change in the vertical effective stress which arises as a result of either excavation or filling. Generally, K_r should be set to $\nu/1-\nu$ but in the situation where σv is being increased to above the preconsolidation pressure a value of K_r of about 1-sin Ø may be more appropriate (Ø = angle of internal shearing resistance).

2.7 Struts or Anchors

Struts or anchors can be installed at any node at any stage during the analysis. As shown in Figure 2 the struts are specified as having a prestress force P_s and a stiffness S_s in terms of force/unit displacement. To model the effect of a moment being applied to the wall by a strut or an anchor a lever arm L_s can also be specified such that the moment is equal to L_s times the force in the strut. This feature is mainly used to model the effect of an inclined strut or anchor applying the force eccentrically to the wall section.

The struts are incorporated into the analyses by modifying the wall stiffness (see section 2.3) as follows:

Set

$$[F_s] = [S_s][\delta] + [P_s] \quad \text{and}$$
$$[M_s] = [L_s][F_s] = [L_s]\,[[S_s][\delta] + [P_s]] \tag{10}$$

where $[F_s]$ and $[M_s]$ are the nodal strut forces and moments and $[S_s]$, $[P_s]$ and $[L_s]$ are the nodal strut stiffnesses, prestress forces and lever arms.

Therefore from section 2.3 it follows that

$$[P] = [A]^T[\Theta] + [C][\delta] + [F_s]$$
$$[M] = [L_s][F_s] = [A][\delta] + [B][\Theta] \tag{11}$$

By substitution $[\Theta]$ can be eliminated to give a new stiffness matrix for the wall and struts $[S_1]$ equal to

$$[C] + [S_s] + [A]^T[B]^{-1}\left\{[S_s][L_s]-[A]\right\} \tag{12}$$

In subsequent stages of construction the applied node forces due the struts or anchors are calculated as

$$\left\{[P_s] + [S_s][\Delta]\right\}\left\{[I] + [A]^T[B]^{-1}[L_s]\right\} \tag{13}$$

where $[\Delta]$ are the nodal displacements that have occurred since each strut was installed. This process is equivalent to calculating a set of nodal forces that produce the same effect on the wall as the applied moment at a single node.

2.8 Surcharges

The modelling of surcharges is often required to include the effect of nearby foundations, rafts, etc. In the analysis two types of surcharges can be specified to act on either side of the wall at any stage during construction. They are illustrated in Figure 10 and are a uniformly distributed load (UDL) and a strip load of finite width B acting a distance A from the wall with a pressure q.

Both types of surcharge can be applied at or below the ground surface but the analysis assumes that a surcharge has no effect above its level of application.

The procedure required to incorporate the effects of the surcharges can be divided into two steps:

(a) compute the changes in earth pressures which would occur if the nodes do not move (i.e. an unyielding wall),

(b) compute the changes in the active and passive limits for the earth pressures.

Both of these steps are problematic, and they will be discussed in turn.

(a) Stress Changes for unyielding wall

For the case of a UDL the horizontal stress change below the surcharge is simply evaluated as qK_r. For a strip load the change in stress is difficult to determine because the horizontal stress is extremely sensitive to the variation with depth of the soil stiffness. Two extremes may be considered.

(1) The stiffness is relatively constant for a depth several times greater than the width of the footing. In this case, the Boussinesq equations may be used to derive horizontal stresses in the ground. The

pressures on a rigid (ideally frictionless) vertical boundary would be double the Boussinesq values, and this fact can be used to estimate the pressures on the wall before further movement takes place.

(2) The stiffness increases sharply at a depth less than the width of the footing. In this case the load will appear to the soil to act rather like a UDL.

The analysis calculates the change of pressure on the wall before further movement using the equation

$$p = 2K_s \Delta \sigma_{hB} \qquad (14)$$

where $\Delta \sigma_{hB}$ = change of horizontal stress according to the Boussinesq equations

K_s = a correction factor specified by the user.

For case (1) above, K_s should be 1.0. For other cases K_s can have a large range of values, the evaluation of which is beyond the scope of the analysis. If the strip load is wide compared with its distance from the wall and the depth of the deforming soil, a value of $K_s = \nu/(1-\nu)$ will give results equivalent to loading with a UDL with $K_r = \nu/(1-\nu)$.

Initial surcharges, which are present before construction of the wall, are modelled in the same way as other surcharges. However, in selecting K_s the effects of construction of the wall on existing horizontal stresses must be considered.

(b) Active/passive pressure limits

The effect of a UDL on the active/passive pressures are simply calculated as qK_a and qK_p respectively. For a strip load the effect is difficult to determine and depends on many factors.

In order to formulate a relatively simple approximation to the "correct" solution for the active pressure case parametric studies have been carried out using straight line and log spiral shaped failure surfaces. Only soil that has constant properties with depth has been considered. The ranges of variables considered were as follows; ϕ from 15 to 60°, $q/\gamma B$ from 0.33 to 5 and A/B from 0 to 2. The results showed that the straight line and log spiral methods usually gave very similar results. It is considered important that whatever system is chosen should be generally conservative. In the

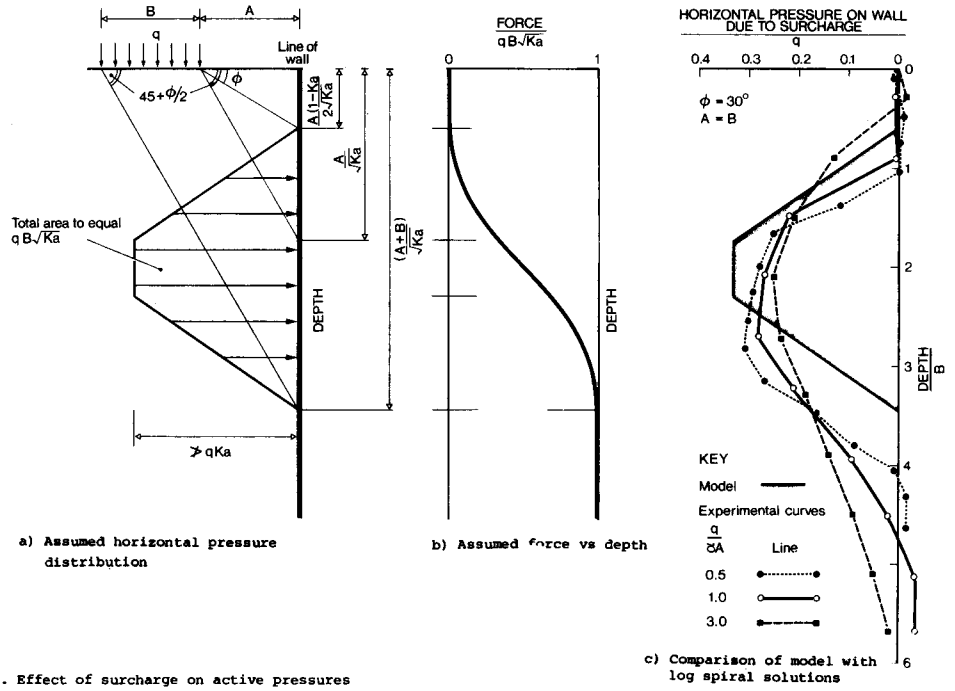

a) Assumed horizontal pressure distribution

b) Assumed force vs depth

c) Comparison of model with log spiral solutions

Fig 11. Effect of surcharge on active pressures

case of active pressure this should be achieved by maximising the pressure near the top of the soil.

From purely theoretical considerations the approximation illustrated in Figure 11 was developed to represent the active pressure distribution. Figure 11(a) shows the shape of the pressure diagram and the criteria for calculating it; if the width of the load (B) is small the diagram will become triangular. The pressure shown in Figure 11(a) develops the force shown against depth in Figure 11(b). A comparison between the theoretical pressure distribution and several curves taken from the parametric study is presented in Figure 11(c). It is seen that the theoretical solution agrees well with the "correct" solutions and is generally conservative.

If K_a varies with depth it is considered conservative to choose a mean value of K_a between any depth z and the ground surface and then impose the criteria that the active force due to the surcharge down to depth z be equal to the force derived from the diagram in Figure 11(b). This is subject to the further limitation that the pressure never exceeds qKa at any depth.

The effects of a strip load on the passive pressure are not as easily represented by a simple pressure diagram. It is generally conservative to force the increased resistance as low as possible, but in some instances, for example when a floor slab is preventing toe failure of a wall, it is not. In the light of this the effect on the passive pressure limits due to a strip load must be specified directly.

3 THE PROGRAM - INPUT, OUTPUT

The analysis described in the previous section has been incorporated into a computer program. This program is used by many designers and consequently the input and output facilities of the program are important.

The input to the program is completely interactive. The data is inserted in steps that represent stages of construction and for each action command the program prompts for every variable. Where possible the value is checked to ensure that it is reasonable or indeed possible. At the end of each stage of construction the program produces a complete set of results comprising earth pressures, displacements, and the wall shear forces and bending moments. These can be presented graphically as shown in

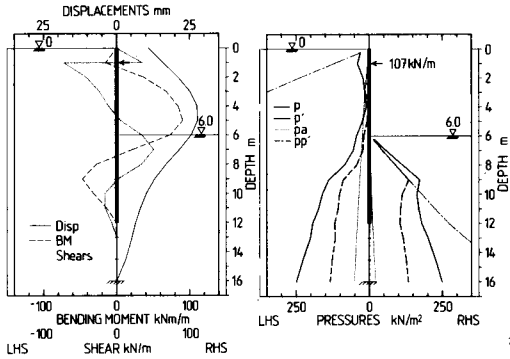

Fig 12. Example of program output

Figure 12 which shows the same problem presented in Figure 7. Figure 12 displays results for the finite element flexibility method with allowance for arching.

4 EXAMPLES

To demonstrate how the analysis can be applied three examples are included in the following sub-sections. The first is a classical problem performed to check the suitability of the analysis. The second is a case where predictions were made during the design and subsequently displacements were measured during construction. Finally, the third case is an unusual problem included to illustrate the versatility of the analysis.

4.1 Rotation of a rigid wall

In 1934 Terraghi reported the results of a now classical series of tests on the lateral pressures of dry sand against a retaining wall. A rigid wall was rotated abouts its base and the changes of earth pressure on the wall were recorded. The results of the tests together with some additional tests performed at Princeton are presented in NAVFAC DM7 (1971) and are redrawn on Figure 13(b). This problem was modelled by the analysis using the geometry and soil properties shown in Figure 13(a). The results are presented in terms of the ratio K in Figure 13(b) where K is derived from the horizontal force (P_H). This force is calculated assuming that it acts at a third of the wall height above the base and gives a moment equal to the moment due to the calculated earth pressures.

The results of the analysis give very similar results to those reported. In

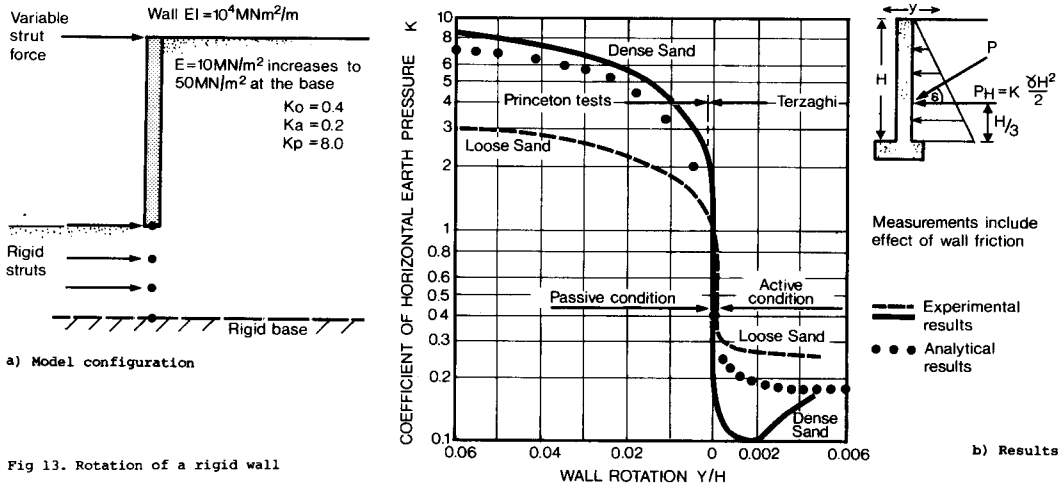

Fig 13. Rotation of a rigid wall

particular a smooth curve is computed for the variation of K with rotation, despite the use of a simple linear elastic/plastic model. This occurs because plastic yield is at first local to the top of the wall and generally spreads downwards.

4.2 A multiply strutted excavation in soft clay

This problem is illustrated in Figure 14(a). At the site about 4m of fill overlies 26m of soft or firm clay over stiff to hard clay. Undrained shear strengths measured by a shear vane for the soft clay are given on the figure. Predictions were made for the excavation assuming a c_u/p_v ratio of 0.25 to represent the strength properties of the clay. To represent the stiffness of the clay an E/c_u ratio of 750, when modelling the early stages of the construction reducing to 75 in the final stage was used. The other parameters used in the analysis are given in Figure 14(a).

The wall displacements predicted for each stage of construction are given in Figure 14(b). The earth pressures for the final stage of analysis are shown in Figure 14(c). These show that arching is predicted below the excavation level on both sides of the wall with the pressure reducing below p_a to the left of the wall and increasing above p_p to the right.

Since the predictions were made the excavation has progressed from stage 0 to stage 4 as shown in Figure 14(a). Inclinometers installed along the line of the wall were used to measure displacements which have been published by Davies and Walsh (1983). These are shown for each stage in Figure 14(b). It can be seen that the predicted and measured displacements agree quite well for construction stages 2 and 3 but for the final stage they do not appear to agree well. This is mainly due to the base of the wall moving much less than predicted. In the design prediction the layer of firm to stiff clay was modelled as being soft clay since there was some doubt about the continuity of this layer. Therefore it was considered sensibly conservative to ignore it. Another prediction was made with the undrained shear strength of the clay increasing to 100kN/m² below a depth of 18m. The final displacements for this case are also shown in Figure 14(b) and agree well with those measured. Underprediction of displacements near the top of the wall are considered to results from the use of stiffer struts than those used in construction.

For the purposes of design, however, this analysis is quite acceptable. The magnitudes of the displacements, and wall bending moments are well predicted. It is these parameters that influence the choice of wall type, excavation procedure and strutting arrangement.

4.3 Short wall restrained by a slab

A further example is illustrated in Figure 15. Figure 15(a) shows the stages of construction which consist of a general excavation of 9.5m followed by the installation of a contiguous bored pile retaining wall. Subsequently a raft is cast to one side of, and directly connected to, the top of the wall. Finally, a further excavation of 7m to the right hand side of the wall allows the installation of a lower level raft.

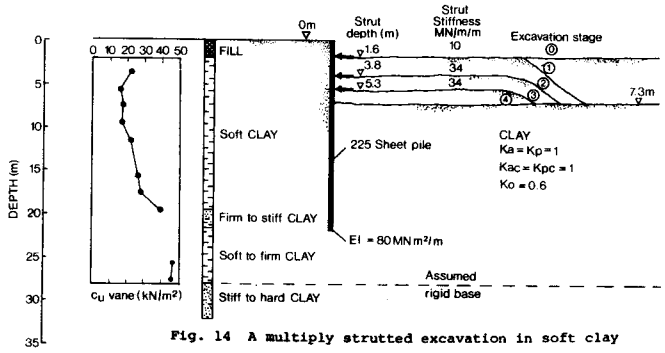

Fig. 14 A multiply strutted excavation in soft clay

a) Details of excavation

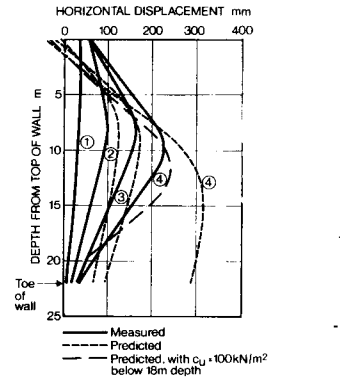

b) Results

c) Predicted earth pressure at stage 4

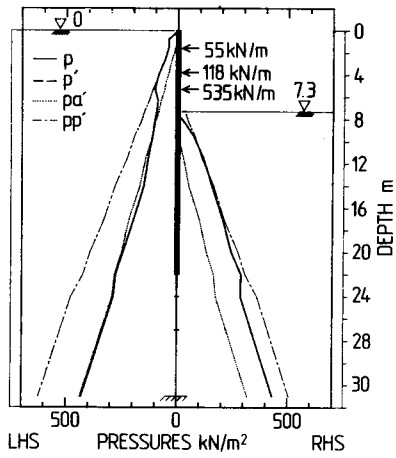

The behaviour of the wall during the 7m excavation is the subject of this example. The parameters used to represent the wall, the soil and the upper raft are given in Figures 15(b) and 15(c). The high initial stresses acting on the wall were obtained by considering the probable soil stress paths. This allowed for drainage during the first part of the 9.5m excavation but for all subsequent excavation the soil was assumed to be undrained. The bending resistance and horizontal restraint of the raft was represented as 3 struts acting on the top three nodes. The wall stiffness (EI) was also increased for the depth of the raft. The results of the analysis are given in Figure 15(d). It can be seen that rotation of the wall is predicted about the top connection with a maximum deflection of 18mm near the base and a maximum bending moment of about 500MNm/m.

During construction it is planned to monitor movements of the wall for comparison with the predictions.

5 VALIDATION

In the previous sections an analysis method has been presented and examples given of its use. However, to be of use it is necessary to determine the reliability of the analysis in predicting the required design parameters.

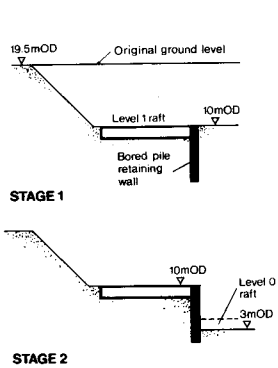

a) Stages of construction

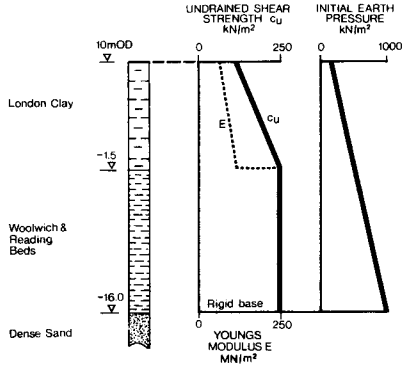

b) Soil properties for stage 2 analysis

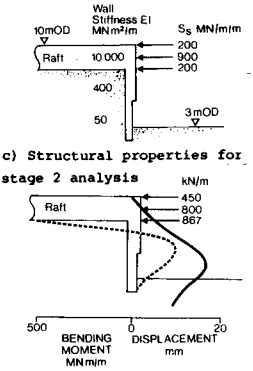

c) Structural properties for stage 2 analysis

d) Predicted behaviour at stage 2

Fig 15. Boared pile wall in London clay

Validation by comparison with actual results is a difficult process. The parameters used in the analysis clearly control the predicted behaviour. For a "back" analysis of a problem with a known result it is usually possible to match the measured response by manipulating the parameters. This does not directly test the analysis itself. However "back analysis" does allow an assessment to be made of the sensitivity of the analysis to the parameters.

An improvement on a "back" analysis is a design prediction which is subsequently verified by measurement. Section 4.2 presented an example of this where it is seen that the design prediction for the actual problem was rather poor. However, the consequences of this error in prediction were not significant. The designer was not trying to achieve exact predictions but rather to explore what may happen. The differences between predictions and measurements in this instance are, therefore, quite acceptable.

Several attempts have also been made to test the program against "correct" solutions. An example has been given in Section 4.1 for a rigid wall rotating about its base. Here the analysis was able to accurately model the measured behaviour. Comparisons have also been made between predictions from this analysis and those using the finite element technique. No examples are given here but generally reasonable agreement is found between the two methods.

Thorough validation of a method of analysis of this type is difficult to achieve.

6. EFFECTS BEYOND THE SCOPE OF THE ANALYSIS

The analysis cannot directly model the effects of parameters that change with time. A common example is a retaining wall in stiff clay where in the short term the soil will behave in an undrained manner but in the long term drained behaviour of the soil is relevant. The wall and permanent strutting system are usually installed quickly with the behaviour of the clay being essentially undrained. The question remains as to how much the strut loads will increase as the soil reaches the long term condition. The increases in strut loads are a function of the changes in pressure acting on the wall resulting from dissipation of excess pore pressures developed within the soil due to excavation. The analysis cannot calculate these changes and the designer must specify them to enable the analysis to model their effect. Creep, another example of a time dependent behaviour, can be significant in both concrete and soil. The analysis cannot directly model the effects of this phenomenon.

Non linear behaviour is also not directly modelled by the analysis. A linear elastic/plastic model is used for the soil but in reality soil is always non linear. If this effect is significant, suitable finite element methods should be used.

The wall itself may also behave in a non linear manner. If required, however, a simple linear elastic/plastic model could be included in the analysis presented here.

7 SUMMARY

1. A numerical method of analysis for flexible retaining walls that is sufficiently simple and cheap to be used in the general design process has been presented.

2. The unusual but very powerful features of the analysis are the ways in which soil stiffness and earth pressure limits are modelled.

3. The soil stiffness is generated from considering a block of elastic material rather than the commonly used series of independent springs.

4. The earth pressure limits are determined from consideration of forces resisted by or applied to the soil rather than simple comparisons with active and passive pressure limits.

5. The importance of good input and output facilities is emphasised.

6. Examples have been given to demonstrate the use and range of the analysis.

7. Thorough validation of the analysis is difficult.

8 ACKNOWLEDGEMENTS

The authors wish to acknowledge the efforts of their many colleagues who have contributed to the development and testing of the computer program based on the analysis presented here.

References

Vaziri, H., B. Simpson, J.W. Pappin and L. Simpson 1982. Integrated forms of Mindlin's equations. Vol. 32, No. 3 Geotechnique. ICE London.

Davies, R.V. and N.M. Walsh 1983. Excavations in Singapore marine clay. Int. Seminar on Construction Problems in Soft Soils. Nanyang Technological Inst., Singapore.

NAVFAC - DM7 1971, Design Manual. US Naval Pubs. and Forms Cntr., Philadelphia Pa. 19120 U.S.A.